Supporting Information for

Plasma-enhanced chemical vapor deposition of amorphous carbon molecular sieve membranes for gas separation

Hiroki Nagasawa, Masakoto Kanezashi, Tomohisa Yoshioka and Toshinori Tsuru

Department of Chemical Engineering, Hiroshima University, Higashi-Hiroshima, Hiroshima 739-8527, Japan

ESI-1

Experimental

Membrane preparation: Amorphous carbon membranes were fabricated onto a porous α-alumina capillary tube (average pore size, 150 nm; outer diameter, 3 mm; length, 30 mm; supplied by NOK, Corp., Japan) with a nanoporous intermediate layer. The procedure for the preparation of the intermediate layer was as follows: First, a TiO_2 sol was coated onto the surface of a porous support, and the support was fired at 550°C to form a TiO_2 layer with an average pore size of 4-5 nm. Subsequently, a SiO_2-ZrO_2 sol was coated onto the TiO_2 layer and fired at 550°C to form a SiO_2-ZrO_2 intermediate layer, which a pore size of approximately 1 nm.

An amorphous carbon thin layer was deposited onto the SiO_2-ZrO_2 intermediate layer *via* plasma-enhanced chemical vapor deposition (PECVD). Figure S1 shows a schematic diagram of the PECVD equipment. A plasma reactor consisted of a quartz tube surrounded by a RF coil. The tubular support was placed 3 cm downstream of the RF coil. Prior to the plasma-deposition, the reactor was vacuumed to 10 Pa, and propylene as a carbon precursor was fed to the reactor at a fixed-flow rate of 10 sccm. The propylene plasma was generated with a 13.56 MHz RF source (AX-300III, AD-TEC, Japan) at 50 W. The film samples for FT-IR and Raman spectroscopy were prepared on a silicon wafer under the same deposition conditions that were used for the membrane preparation.

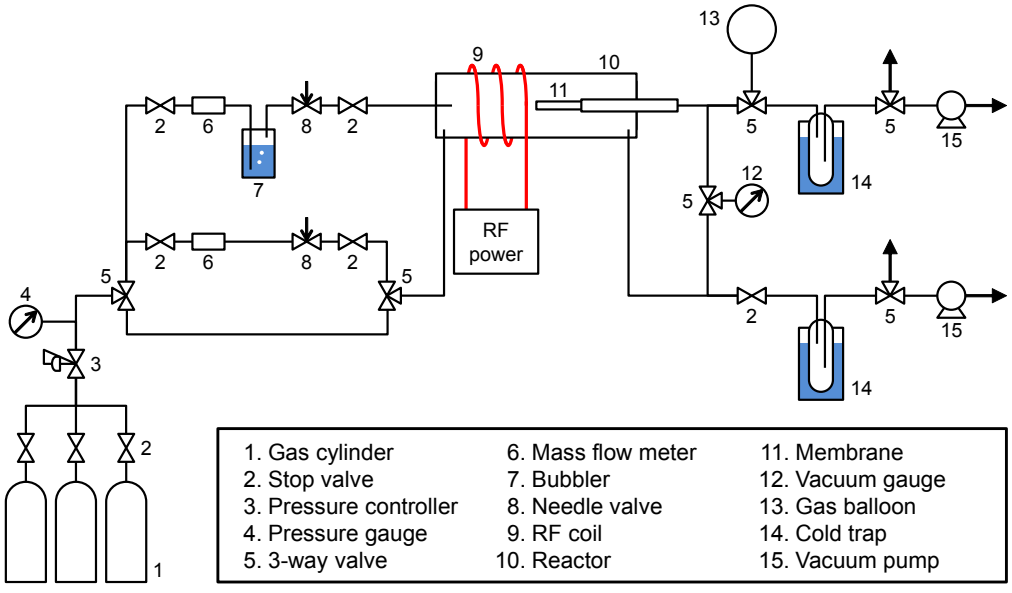

Figure S1. Schematic diagram of the PECVD equipment.

Film characterization: The structure of the PECVD-derived thin layer was analyzed using field-emission scanning electron microscopy (FE-SEM, Hitachi S-4800), Fourier-transform infrared spectroscopy (FTIR, JASCO FT/IR-4100), and Raman spectroscopy (Renishaw inVia Reflex/StreamLine microRaman spectrometer).

Gas permeation measurement: The gas permeation properties of the PECVD-derived amorphous carbon membranes were evaluated using the same equipment as that used for the plasma-deposition. The permeances were measured using the constant-volume variable-pressure method. The permeate side of the membrane was vacuumed to 10 Pa prior to the measurement. The pressure of the feed, p_1, was kept at 105 kPa, and the pressure in the permeate, p_2, was measured using a pressure transducer (MKS Baratron type 722A). By measuring the time course of the pressure in the permeate, the single gas permeance, P, was determined from the following equation:

$$P = \frac{V_2}{ART\Delta t} ln \frac{(p_1 - p_{2,1})}{(p_1 - p_{2,1})} \quad \text{(Eq. 1)}$$

where V_2 is the fixed volume of the permeate side, A is the surface area of the membrane, R is the gas constant and T is the absolute temperature of the gas balloon. The fixed volume, V_2, including gas balloon was 5.05×10^{-4} m^3. The $p_{2,1}$ and $p_{2,2}$ indicate the pressure in the permeate at $t = 0$ and t = Δt, respectively.

ESI-2

Film characterization of PECVD-derived amorphous carbon films

The rate of film deposition was investigated using the time dependence of FTIR spectra. Figure S3 is the peak area of the asymmetric stretching of C-H groups at 2800-3000 cm^{-1} as a function of plasma deposition time. It is apparent that the peak area increased linearly as the deposition time extended. The absorption peak area represents the mean thickness of plasma deposited layers. Thus, this result indicates that the deposition amount of the films increases linearly with the increasing deposition time. This linear trend of film growth was consistent with our previous results for the fabrication of siloxane-based membranes.[S1]

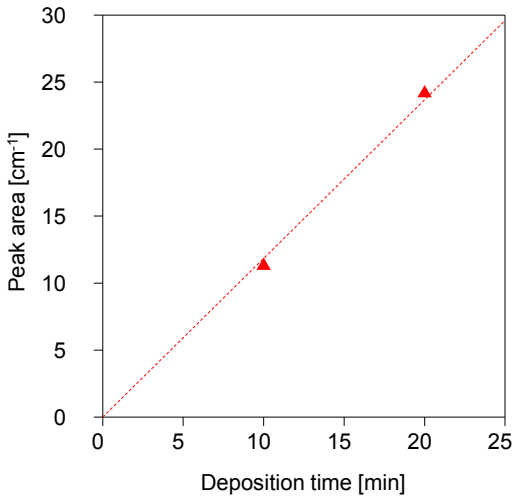

Figure S2. Peak area the asymmetric stretching of C-H groups at 2900-3000 cm^{-1} of PECVD-derived amorphous carbon films as a function of deposition time.

The film structure was further investigated by XPS analysis. Figure S4 shows the survey spectra of the PECVD-derived amorphous carbon film. The spectra shows the presence of carbon as well as oxygen and nitrogen. The origin of these oxygen and nitrogen might be the impurity in the feed gas and/or from the ambient air. Since a number of active sites still remain after plasma-deposition, the surface of the film can easily react with the species in the atmosphere. The atomic concentrations of carbon, oxygen, and nitrogen, calculated from the peak areas of these elements and their sensitivity factor, were 89.3% (C), 9.1% (O), and 1.6% (N), respectively. High resolution XPS spectra for C_{1s}, as shown in Figure S5, showed a sharp peak at 284.2 eV which is ascribed to C-C, C=C, and CH_x, The shoulder at the higher binding energy side of the peak suggests the presence of a small amount of C-O and C=O. The results indicate that the film is mainly composed of hydrogenated amorphous carbon.

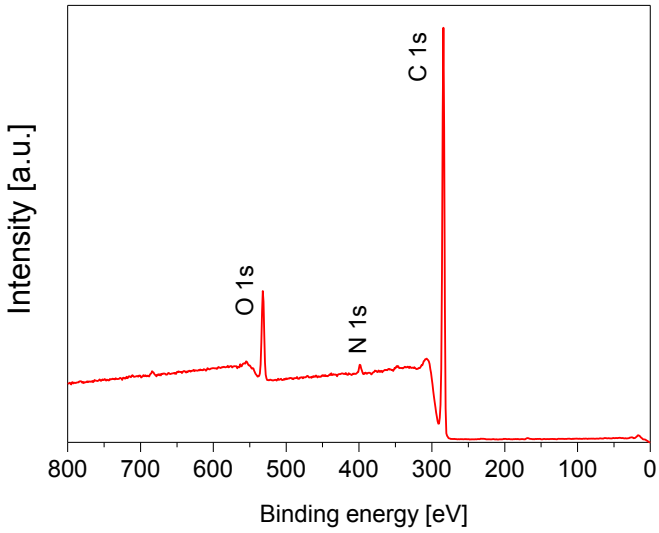

Figure S3. Survey XPS spectra for PECVD-derived amorphous carbon film.

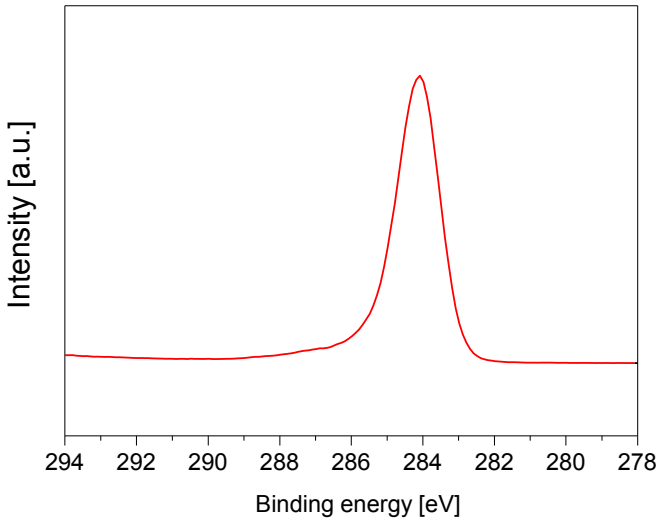

Figure S4. High resolution XPS spectra for C_{1s} for PECVD-derived amorphous carbon film.

ESI-3

Modified gas-translation model

The gas-translation (GT) model, which describes the gas permeation through microporous media was originally proposed by Xiao and Wei,[S2] and Shelekhin *et al*.[S3] According to the GT model, the gas permeance for the *i*-th component, P_i, through the microporous membrane can be expressed by Eq. 2.

$$P_i = \rho_{g,i}\frac{\varepsilon}{\tau L}d_e\sqrt{\frac{8}{\pi M_i RT}}exp\left(-\frac{E_{P,i}}{RT}\right) \quad \text{(Eq. 2)}$$

where $\rho_{g,i}$ is the geometrical probability of diffusion for the *i*-th component, ε is the porosity, τ is the tortuosity, L is the thickness, d_e is the effective diffusion length, M_i is the molar weight of the *i*-th component, R is the gas constant, T is the absolute temperature, and $E_{P,i}$ is the activation energy of permeation for the *i*-th component. It should be noted that, in the GT model, the effective diffusion length was assumed to be the pore diameter, d_p, and the size of permeating molecules, d_i, was not considered. Recently, a modified GT model, which considered the size of permeating molecules and assumed the effective diffusion length to be $(d_p - d_i)$ instead of d_p, was proposed.[3, 4] In the modified GT model, the geometrical probability, $\rho_{g,i}$, is defined as the product of (1) the random factor (1/3) of a 3-D space and (2) the ratio of the effective cross-sectional area of a pore for the *i*-th component, A_i, over the physical cross-sectional area of the pore, A_0, as follows:

$$\rho_{g,i} = \frac{1}{3}\frac{A_i}{A_0} = \frac{1}{3}\frac{\pi(d_p - d_i)^2/4}{\pi d_p^2/4} = \frac{1}{3}\frac{(d_p - d_i)^2}{d_p^2} \quad \text{(Eq. 3)}$$

By introducing the modified effective diffusion length, $(d_p - d_i)$, and Eq. 3 into Eq. 2, the permeance based on the modified GT model can be expressed as follows:

$$P_i = \frac{\varepsilon}{3\tau L}(d_p - d_i)\frac{(d_p - d_i)^2}{d_p^2}\sqrt{\frac{8}{\pi M_i RT}}exp\left(-\frac{E_{P,i}}{RT}\right) \quad \text{(Eq. 4)}$$

$$= \frac{k_{0,i}}{\sqrt{M_i RT}}exp\left(-\frac{E_{P,i}}{RT}\right) \quad \text{(Eq. 5)}$$

Where $k_{0,i}$ is the pre exponential factor defined as follows:

$$k_{0,i} = \frac{\varepsilon}{3\tau L}\frac{(d_p - d_i)^3}{d_p^2}\sqrt{\frac{8}{\pi}} \quad \text{(Eq. 6)}$$

The activation energy of permeation, $E_{P,i}$, can be obtained by regression using Eq. 5 with the experimentally obtained temperature dependence of the single gas permeance. It is interesting to note that Eq. 5 covers the activated diffusion ($E_{P,i} > 0$), surface diffusion ($E_{P,i} < 0$), and Knudsen diffusion ($E_{P,i} = 0$): Assuming that the homogeneous potential field exists inside the micropores, the activation energy of permeation can be interpreted as the sum of the activation energy of diffusion for permeating molecules to overcome the potential barrier, and the energy of interaction with the pore walls. For permeation through the small micropores, where the diffusion barrier limits the permeation, the apparent activation energy is $E_{P,i} > 0$, and is referred to as the activated diffusion. For permeation through the larger micropores, where the diffusion barrier is decreased but the interaction with the pore walls still has a profound effect on permeation, the apparent activation energy is $E_{P,i} < 0$ and is referred to as the surface diffusion. Moreover, for permeation through much larger micropores, where the effects of the diffusion barrier and interaction with the pore walls can be negligible, the Knudsen diffusion mechanisms become dominant

and the apparent activation energy becomes $E_{P,i} = 0$.

ESI-4

Normalized Knudsen-based permeance (NKP) analysis [S4,S5]

Based on the modified GT model, the NKP method was proposed as a simple method for the determination of membrane pore sizes of less than 1 nm. NKP, f_{NKP}, is the ratio of the experimentally obtained permeance of the *i*-th component over the ideal Knudsen permeance of the *i*-th component that was estimated from the permeance of a standard gas as given in Eq. 7.

$$f_{NKP} = \frac{P_i}{\sqrt{\frac{M_S}{M_i}} P_S} \quad \text{(Eq. 7)}$$

where the subscription "S" represents a standard gas: for example, helium, which is the smallest gas molecule. By introducing Eq. 4, Eq. 7 can be rewritten as follows:

$$f_{NKP} = \frac{P_i}{\sqrt{\frac{M_S}{M_i}} P_S} = \frac{(d_p - d_i)^3}{(d_p - d_S)^3} exp\left(-\frac{E_{P,i} - E_{P,S}}{RT}\right) \quad \text{(Eq. 8)}$$

Assuming that (1) all gas species permeate through an identical pore size, and (2) the difference in activation energy for permeation is negligible, Eq. 8 can be simplified as follows:

$$f_{NKP} = \frac{P_i}{\sqrt{\frac{M_S}{M_i}} P_S} = \frac{(d_p - d_i)^3}{(d_p - d_S)^3} \quad \text{(Eq. 9)}$$

The pore size effective for gas permeation can, therefore, be estimated by best fitting the experimentally obtained f_{NKP} with Eq. 9. Figure S2 shows the f_{NKP} at 200°C for a PECVD-derived amorphous carbon membrane as a function of kinetic diameter. The f_{NKP} for CO_2 was larger than unity, indicating that the permeance of CO_2 was larger than that supposed by the modified GT model. This was due to the large affinity of CO_2 with the pore surface, which caused a concentration enhancement in the micropores. The solid curve indicates the best fit of f_{NKP} calculated from Eq. 9. The pore size effective for gas permeation was estimated to be 0.53 nm. The pore size was between the molecular size of N_2 and SF_6. This result indicates, as mentioned in the main text, that the permeation of He, H_2, CO_2, and N_2 occurs through the amorphous carbon matrix, whereas the permeation of SF_6 occurs through grain boundaries. The plasma-deposited amorphous carbon layer consisted of micropores with the size which was suitable for gas separation.

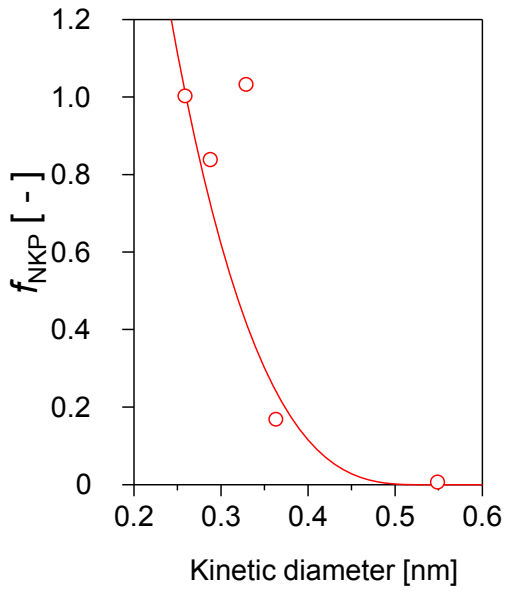

Figure S5. Normalized Knudsen-based permeance, f_{NKP}, at 200°C for PECVD-derived amorphous carbon membrane as a function of kinetic diameter. Symbols, experimental; solid curve, calculated based on Eq. 9.

References

S1 H. Nagasawa, H. Shigemoto, M. Kanezashi, T. Yoshioka, T. Tsuru, *J. Membr. Sci.*, 2013, **441**, 45.

S2 J. Xiao, J. Wei, Chem. Eng. Sci., 1992, **47**, 1123.

S3 A. B. Shelekhin, A. G. Dixon, Y. H. Ma, AIChE J., 1995, **41**, 58.

S4 H. R. Lee, M. Kanezashi, Y. Shimomura, T. Yoshioka, T. Tsuru, AIChE J., 2011, 57, 2755.

S5 T. Yoshioka, M. Kanezashi, T. Tsuru, AIChE J., 2013, 59, 2179.